nature biomedical engineering

ARTICLES

PUBLISHED: 28 NOVEMBER 2016 | VOLUME: 1 | ARTICLE NUMBER: 0002

A brush-polymer/exendin-4 conjugate reduces blood glucose levels for up to five days and eliminates poly(ethylene glycol) antigenicity

Yizhi Qi[1], Antonina Simakova[2], Nancy J. Ganson[3], Xinghai Li[1], Kelli M. Luginbuhl[1], Imran Ozer[1], Wenge Liu[1], Michael S. Hershfield[3,4], Krzysztof Matyjaszewski[2] and Ashutosh Chilkoti[1*]

The delivery of therapeutic peptides and proteins is often challenged by short half-lives and the consequent need for frequent injections that limit efficacy, reduce patient compliance and increase treatment cost. Here, we demonstrate that a single subcutaneous injection of site-specific (C-terminal) conjugates of exendin-4 (exendin)—a therapeutic peptide that is clinically used to treat type 2 diabetes mellitus—and poly[oligo(ethylene glycol) methyl ether methacrylate] (POEGMA) with precisely controlled molecular weights lowered blood glucose for up to 120 h in fed mice. Most notably, we show that an exendin-C-POEGMA conjugate with an average of nine side-chain ethylene glycol (EG) repeats exhibits significantly lower reactivity towards patient-derived anti-poly(ethylene glycol) (anti-PEG) antibodies than two US FDA-approved PEGylated drugs, and that reducing the side-chain length to three EG repeats completely eliminates PEG antigenicity without compromising *in vivo* efficacy. Our findings establish the site-specific conjugation of POEGMA as a next-generation PEGylation technology for improving the pharmacological performance of traditional PEGylated drugs, whose safety and efficacy are hindered by pre-existing anti-PEG antibodies in patients.

Therapeutic peptides and proteins are an important class of drugs, with more than 100 peptides and proteins approved by the US FDA to treat various diseases and many more in clinical and pre-clinical development[1,2]. However, the clinical use of all peptides and most proteins (with the exception of antibodies, albumin[3] and transferrin[4]) is challenged by their short plasma half-life, necessitating frequent injections, which can cause an undesirable peak-to-valley fluctuation of the drug concentration *in vivo* as well as reduce patient compliance and increase treatment cost[5]. Other limitations of peptide and protein therapeutics may include poor stability, low solubility and immunogenicity[6]. To address these limitations, various delivery strategies have been developed for the sustained delivery of peptide and protein therapeutics, ranging from particulate systems and depots, to chemical conjugation with long-circulating polymers such as PEG, to recombinant fusion with long-circulating proteins such as albumin or the fragment crystallizable (Fc) domain of antibodies[7,8].

PEGylation, or the covalent conjugation of therapeutic peptides and proteins (and more recently nucleotide-based drugs) with the 'stealth' polymer PEG, is one of the most widely used approaches to increase the circulation half-life and stability and to reduce the immunogenicity of these therapeutic biomolecules, as evident from the many PEGylated drugs approved by the FDA and the numerous others in development[6,9,10]. However, after close to four decades of research and over two decades of clinical use, the drawbacks of PEGylation have begun to emerge. Conventional methods for the synthesis of PEGylated conjugates have notable limitations: (i) conjugation involves the reaction between protein-repulsive PEG chains and biomacromolecules, so that even with a large excess of polymer, steric hindrance still results in a low yield of conjugate, typically in the 10–20% range[11]; (ii) the presence of a large excess of unreacted polymer makes product purification non-trivial; and (iii) conjugation typically involves reacting the chain ends of the polymer with reactive side groups on lysine and cysteine residues, which are often promiscuously distributed on the biomolecule, thus yielding chemically heterogeneous products that can compromise the bioactivity of the drug and greatly complicate regulatory approval[12–15].

Furthermore, the immunogenicity of PEG has recently attracted much attention. Anti-PEG antibodies have been induced in patients treated with some PEGylated enzymes. In clinical trials of PEG-uricase[16,17] and PEG-asparaginase[18], these anti-PEG antibodies have markedly accelerated blood clearance, abrogated clinical efficacy and increased the risk and severity of infusion reactions. Circulating anti-PEG antibodies have also been found in individuals who are naive to PEGylated materials, and are possibly induced by chronic exposure to free PEGs present in commonly used consumer products[19,20]. High levels of such pre-existing anti-PEG antibodies have recently been linked to serious first-exposure allergic reactions to a PEGylated RNA aptamer, which led to the early termination of a clinical trial[21].

To address the synthetic limitations of previous PEG conjugation methodologies, we have previously developed a strategy named sortase-catalysed polymer conjugation[22]. This strategy exploits the C-terminal native-peptide-ligation mechanism of the enzyme sortase A, derived from *Staphylococcus aureus*, to attach a polymerization initiator site specifically and stoichiometrically (1:1) at the C-terminus of a peptide or protein to enable grafting of the PEG-like brush polymer POEGMA from the peptide/protein macroinitiator by *in situ* atom transfer radical polymerization (ATRP) in aqueous buffer[23,24].

Although POEGMA has been grafted from various model proteins and peptides[22,25–29], very few studies have reported POEGMA conjugates of clinically relevant biologic therapeutics for the systematic

[1]Department of Biomedical Engineering, Duke University, Durham, North Carolina 27708, USA. [2]Department of Chemistry, Carnegie Mellon University, Pittsburgh, Pennsylvania 15213, USA. [3]Department of Medicine, Division of Rheumatology, Duke University Medical Center, Durham, North Carolina 27710, USA. [4]Department of Biochemistry, Duke University School of Medicine, Durham, North Carolina 27710, USA. *e-mail: chilkoti@duke.edu

evaluation of the therapeutic potential of this class of conjugates, and conjugation was either carried out post-polymerization[30] or was non-specific[31]. Using our sortase-catalysed polymer conjugation strategy, we grafted POEGMA site-specifically (C-terminal) and stoichiometrically (1:1) from exendin, a peptide drug that is clinically used to treat type 2 diabetes mellitus[32]. We show that a single subcutaneous injection of exendin-C-POEGMA reduces blood glucose for 120 h in fed mice, which is 20 times longer than the reduction resulting from the injection of the unmodified peptide. Most intriguingly, we show that breaking up and appending PEG as short oligomeric side chains of optimized length on the conjugated POEGMA not only retains the long circulation of the POEGMA conjugates but also eliminates their reactivity to patient-derived PEG antibodies. These results demonstrate that the architecture of PEG appended to a biologic drug plays an important role in modulating its antigenicity. This finding is particularly relevant in a clinical context given the growing prevalence of pre-existing anti-PEG antibodies in the general population, which increasingly undermines the safety and efficacy of PEGylated therapeutics. Here, the terms 'antigenicity' and 'immunogenicity' are not interchangeable. Antigenicity is defined herein as the reactivity of an antigen towards pre-existing antibodies in patients, whereas immunogenicity refers to the intrinsic ability of an antigen to generate antibodies in the body.

Results

Sortase-catalysed C-terminal initiator attachment to exendin. We exploited the C-terminal native-peptide-ligation mechanism of sortase A to site-specifically attach the ATRP initiator *N*-(2-(2-(2-(2-aminoacetamido)acet-amido)acetamido) ethyl)-2-bromo-2-methylpropanamide (AEBMP) to the C-terminus of exendin (Fig. 1). A quaternary fusion protein, abbreviated to exendin-srt-His_6-ELP, was recombinantly expressed to serve as the sortase-A substrate (Fig. 1a). As explained in an earlier study[22], 'srt' stands for the native sortase-A recognition sequence LPETG[33], and 'ELP' refers to a stimulus-responsive elastin-like polypeptide that was incorporated to enable easy purification of the fusion protein by inverse transition cycling (ITC, Supplementary Fig. 1a), a nonchromatographic protein purification method that we previously developed[34]. The recognition sequence was deliberately located between the protein and the ELP, so that transpeptidation by sortase A not only attaches the initiator to exendin but also conveniently liberates the purification tag. Sortase A with an N-terminal hexahistidine tag (His_6-tag) was recombinantly expressed from a plasmid constructed in the earlier study[22] and purified by immobilized-metal affinity chromatography (IMAC, Supplementary Fig. 1b). The ATRP initiator AEBMP (Fig. 1) was chemically synthesized with an N-terminal $(Gly)_3$ motif serving as the nucleophile, as maximum reaction rates for sortase-catalysed C-terminal ligation have been reported with two or more glycines[35].

Successful sortase-catalysed initiator attachment (Fig. 1b) resulted in the cleavage of exendin-LPETG-His_6-ELP into exendin-LPET and G-His_6-ELP, followed by the attachment of AEBMP to exendin-LPET to generate the macroinitiator product (exendin-C-Br). Sodium-dodecyl-sulfate–polyacrylamide-gel electrophoresis (SDS-PAGE) analysis of the reaction mixture (Fig. 2a) showed >90% conversion to exendin-C-Br as assessed by gel densitometry. Similar to the previous study[22], a His_6-tag was intentionally inserted between srt and ELP on exendin-srt-His_6-ELP fusion, such that on transpeptidation by His_6-sortase A, all of the residual reactants, enzyme and side products except the desired product—exendin-C-Br—carried a His_6-tag. Consequently, elution through an IMAC column yielded pure exendin-C-Br (Fig. 2a) in the eluent while leaving all other unwanted species bound to the resin.

Synthesis and characterization of exendin-C-POEGMA conjugates. Next, we conducted *in situ* activator regenerated by electron transfer (ARGET)-ATRP[36] to graft POEGMA from exendin-C-Br (Fig. 1c). An OEGMA monomer with an average mass of ~500 Da or approximately nine side-chain EG repeats (EG9) was used, as shown by liquid chromatography electrospray ionization mass spectrometry (LC/ESI-MS) analysis (Supplementary Fig. 2a). The reaction time was varied to produce EG9 exendin-C-POEGMA conjugates with a range of weight-average molecular mass (M_w) values. Size exclusion chromatography (SEC) analysis of exendin-C-Br before polymerization as detected by UV–visible absorbance at 280 nm (Fig. 2b) showed a single peak eluting at 23.7 min. After polymerization, the intensity of the macroinitiator peak greatly diminished and was accompanied by the appearance of peaks at 21.3, 19.5, 17.8, 16.5 and 15.0 min, corresponding to EG9 exendin-C-POEGMA conjugates with increasing M_w as the reaction time was increased. The results from UV–visible detection were in agreement with those from refractive index (RI) detection (Supplementary Fig. 3a). Integration of the peak areas in the UV–visible chromatograms showed that the average conjugation yield was ~80%. As shown in Table 1, the synthesized conjugates had number-averaged molecular mass (M_n) values that ranged from 25.4 to 155.0 kDa, and all conjugates had very narrow dispersities ($Đ \leq 1.15$). The conjugates could be easily and completely purified by a single round of preparative SEC (Supplementary Fig. 3b).

Exendin acts by binding and activating the G protein-coupled glucagon-like peptide (GLP)-1 receptor (GLP-1R), which results in the release of cyclic adenosine monophosphate (cAMP) as a second messenger in a downstream signalling cascade, ultimately leading to the secretion of insulin to regulate blood glucose[37]. The potency of native exendin and the EG9 exendin-C-POEGMA conjugates were next assessed by quantifying the intracellular cAMP release as a result of GLP-1R activation in baby hamster kidney (BHK) cells that were stably transfected with rat GLP-1R. As shown in Fig. 2c and Table 1, grafting EG9 POEGMA from exendin increases the half-maximum effective concentration (EC_{50}) of the peptide in a molecular-weight-dependent manner, which indicates decreased

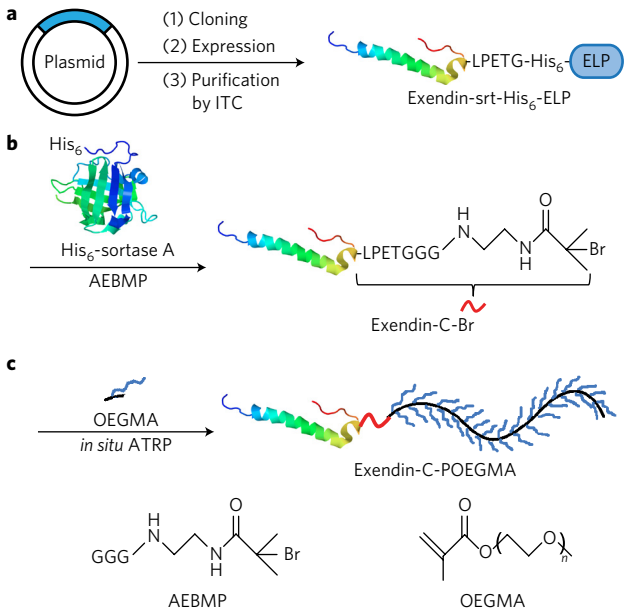

Figure 1 | Synthesis of exendin-C-POEGMA. a, Recombinant expression of the sortase-A substrate, exendin-srt-His_6-ELP, and purification by ITC[34]. **b**, Sortase-catalysed site-specific attachment of AEBMP (structure shown below) to the C-terminus of exendin to generate exendin-C-Br. **c**, *In situ* ATRP of OEGMA (structure shown below) from exendin-C-Br yielding exendin-C-POEGMA. Images from the RCSB PDB of: PDB ID 1T2P (sortase A), ref. 55; PDB ID 1JRJ (exendin-4), ref. 56.

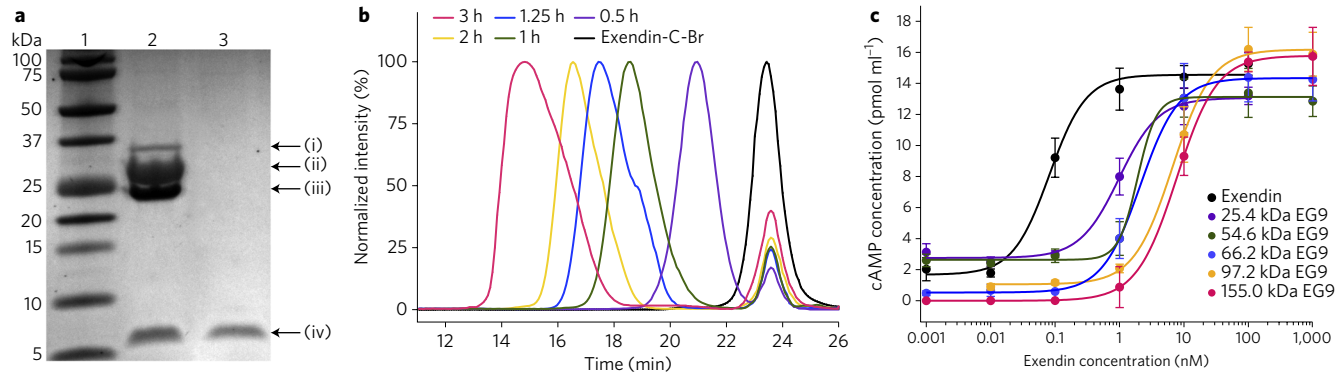

Figure 2 | Characterization of the exendin-C-Br macroinitiator and EG9 exendin-C-POEGMA conjugates. a, Coomassie-stained SDS-PAGE analysis of initiator attachment on exendin by sortase A. Lane 1: M_w marker; lane 2: sortase reaction mixture after 18 h of reaction; lane 3: purified exendin-C-Br macroinitiator. (i) Exendin-srt-His_6-ELP; (ii) cleaved G-His_6-ELP; (iii) His_6-sortase A; (iv) exendin-C-Br. **b**, SEC traces of the ATRP reaction mixtures for grafting EG9 POEGMA from exendin-C-Br carried out for the times indicated, as detected by UV–visible absorbance at 280 nm. **c**, cAMP response of native exendin and EG9 exendin-C-POEGMA conjugates with various M_n values in BHK cells that are expressing the GLP-1R. Results are plotted as the mean ± SEM, $n = 3$. EC_{50} values are summarized in Table 1.

receptor binding with increasing polymer M_w as a result of the steric hindrance imposed by the appended POEGMA chain.

***In vivo* therapeutic efficacy of EG9 exendin-C-POEGMA.** The *in vivo* efficacy of EG9 exendin-C-POEGMA conjugates was assessed in male C57BL/6J mice that were maintained on a 60 kilocalorie (kcal)% fat diet so as to develop a diabetic phenotype[38,39]. A dose-dependent study was first performed to determine an adequate dose. A 66.2 kDa EG9 exendin-C-POEGMA conjugate was administered to mice via a single subcutaneous injection of the conjugate at 25, 50 and 85 nmol kg^{-1} of mouse body weight. Blood glucose levels in fed mice measured at various time points post-injection revealed an overall slight increase in the duration of glucose reduction with increasing doses of the conjugate compared with the PBS control (Supplementary Fig. 4a,b and Supplementary Table 1). A similar trend was observed in the mouse body weights, where the mice treated with the highest dose showed considerably more weight loss than those treated with the two lower doses (Supplementary Fig. 4c). Although the weight-lowering benefit of exendin has been well established[40], overdosing can cause nausea, which can lead to acute weight loss in rodents[41]. The excessive weight loss seen in mice that received the highest dose suggests the possibility of nausea; therefore all subsequent studies used a dose of 25 nmol kg^{-1}.

To investigate the effect of M_w on the glucose regulatory effect of EG9 exendin-C-POEGMA conjugates, native exendin and conjugates of four different M_w values ($M_n = 25.4$, 54.6, 97.2 and 155.0 kDa) were tested at a single subcutaneous injection at 25 nmol kg^{-1} of mouse body weight. While unmodified exendin was only able to lower blood glucose for 6 h relative to the PBS control (Fig. 3a; full glucose profiles are presented in Supplementary Fig. 5), modification with EG9 POEGMA significantly extended the glucose-lowering effect of exendin for up to 120 h, with the onset, magnitude and duration of the effect dependent on M_w (Fig. 3b–e, Supplementary Table 2). As is evident from the overlaid glucose profiles in Supplementary Fig. 6a (overlaid unnormalized glucose profiles are presented in Supplementary Fig. 6b), an increase in M_w delays the onset but prolongs the duration of glucose reduction, and the two higher M_w conjugates showed an overall smaller magnitude of glucose reduction. This trend is also mirrored by the weight profiles of treated animals (Supplementary Fig. 6c). The two higher M_w conjugates also showed much more flat and steady glucose profiles. The glucose profile of the 155.0 kDa conjugate in particular resembled that of a sustained-release depot, with no peak-to-valley effect that can cause undesirable side effects.

The *in vitro* cAMP results and the *in vivo* M_w-dependent glucose measurements in fed mice collectively show that an increase in M_w of the conjugated polymer decreases the potency but increases the circulation duration of the EG9 exendin-C-POEGMA conjugate. We therefore hypothesize that an optimal M_w of the conjugate exists that can best balance these two opposing effects. The area under

Table 1 | Physical properties and biological activity of exendin and exendin-C-POEGMA conjugates.

Species	Reaction time (h)	M_w (Da)	M_n (Da)	$Đ$ (M_w/M_n)	R_h (nm)	EC_{50} (nM)
Exendin			4,186.6*	1.00†	2.2 ± 0.1	0.08 ± 0.01
EG9	0.5	26,400	25,400	1.04	4.5 ± 0.4	0.84 ± 0.09
EG9	1	56,800	54,600	1.04	5.6 ± 0.5	1.91 ± 0.35
EG9	1.25	72,200	66,200	1.09	5.9 ± 0.5	2.10 ± 0.08
EG9	2	100,000	97,200	1.03	6.8 ± 0.7	6.67 ± 0.21
EG9	3	178,000	155,000	1.15	7.6 ± 0.5	7.69 ± 0.04
EG3	3	27,400	26,300	1.04	3.8 ± 0.4	3.29 ± 0.27
EG3	5.5	60,600	55,600	1.09	4.8 ± 0.5	4.17 ± 0.13
EG3	8	82,700	71,600	1.16	5.4 ± 0.6	5.11 ± 0.23

*Calculated from the amino acid sequence. †Default value due to the unimolecular nature of the peptide. M_w and $Đ$ values were determined by SEC-MALS. R_h was measured by dynamic light scattering. The EC_{50} values of the EG9 and EG3 conjugates were derived from the cAMP response curves in Fig. 2c and Supplementary Fig. 7, respectively. R_h and EC_{50} values are reported as mean ± SEM, $n = 10$ for R_h and $n = 3$ for EC_{50}.

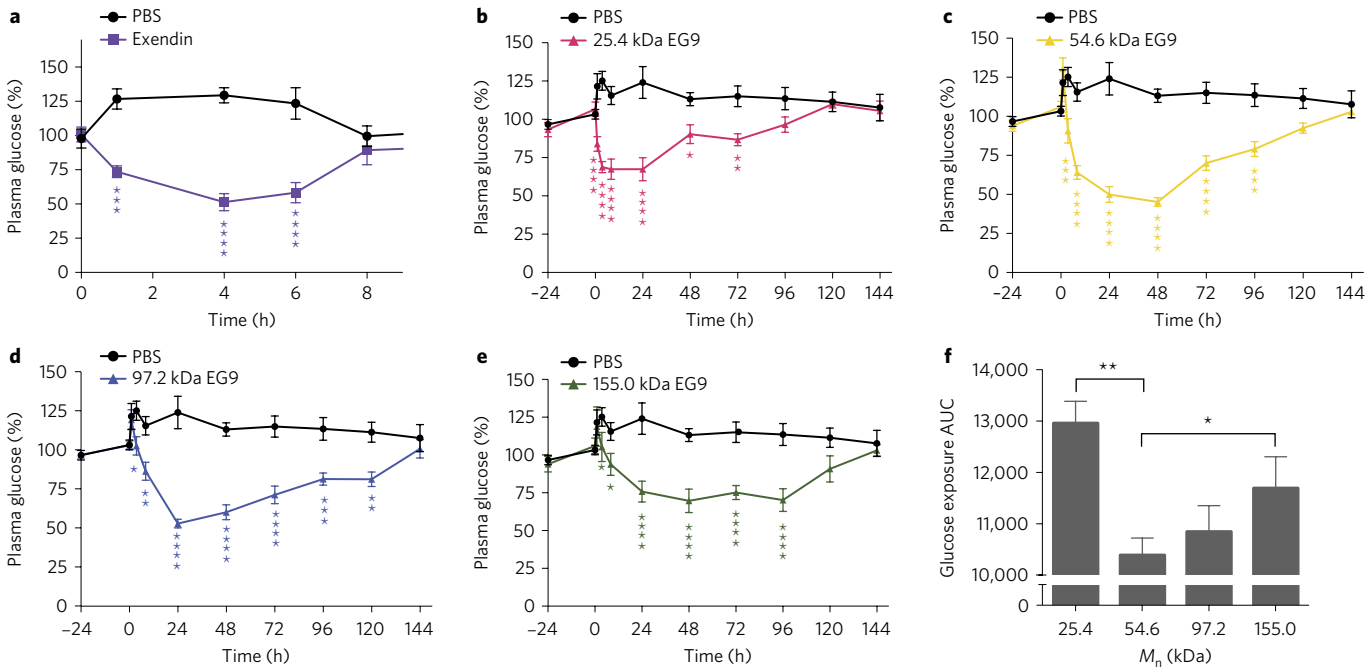

Figure 3 | Assessment of the M_w-dependent *in vivo* efficacy of EG9 exendin-C-POEGMA conjugates. a–e, Blood glucose levels in fed mice were measured before and after a single subcutaneous injection of unmodified exendin (**a**) or 25.4 kDa (**b**), 54.6 kDa (**c**), 97.2 kDa (**d**) and 155.0 kDa (**e**) EG9 exendin-C-POEGMA conjugates compared with the PBS control. The peptide and conjugates were administered at 25 nmol kg^{-1}, and PBS was injected at the equivalent volume, all at $t = 0$ h. Blood glucose levels were normalized to the average glucose levels measured at 24 h before and immediately before injection. Data were analysed by two-way repeated-measures ANOVA followed by *post hoc* Dunnett's multiple comparison test. **f**, AUC of the blood glucose profiles (0 h to 144 h, with respect to the 0% baseline) as a function of conjugate M_n. AUCs were compared using one-way ANOVA followed by *post hoc* Tukey's multiple comparison test. Results are plotted as mean ± SEM, $n = 6$. *$P < 0.05$; **$P < 0.01$; ***$P < 0.001$ and ****$P < 0.0001$.

the curve (AUC) of the glucose profiles in fed mice with respect to a 0% baseline signifies total glucose exposure, which accounts for both the magnitude and the duration of the glucose reduction, and is therefore a manifestation of the combined effect of the two opposing factors. Plotting the AUC of glucose levels as a function of conjugate M_n yielded a roughly inverted bell-shaped distribution with a minimum at 54.6 kDa (Fig. 3f). This suggests that the 54.6 kDa conjugate is optimal among the tested EG9 conjugates in terms of balancing receptor activation potency and sustained duration of action. We thus investigated the 54.6 kDa EG9 conjugate further in subsequent experiments.

To validate the results from the glucose measurements and to obtain further evidence of the efficacy of EG9 exendin-C-POEGMA conjugates, we performed an intraperitoneal glucose tolerance test (IPGTT) at 24 h and 72 h after a single subcutaneous injection of the 54.6 kDa EG9 conjugate or of unmodified exendin at 25 nmol kg^{-1}. IPGTT confirmed the prolonged presence of the conjugate in circulation and its significant effect on glycaemic control: at 24 h post-injection, the AUC of blood glucose level over 2 h after glucose challenge was reduced by 68% ($P < 0.0001$, Fig. 4a) and at 72 h post-injection the AUC was reduced by 48% for conjugate-treated mice compared with PBS controls ($P < 0.01$, Fig. 4b). This is in stark contrast to the unmodified exendin group, which was insignificant at both time points (Fig. 4c and d).

Antigenicity of EG9 exendin-C-POEGMA conjugates. We tested the reactivity of the 54.6 kDa EG9 exendin-C-POEGMA conjugate to anti-PEG antibodies in plasma samples of patients previously treated with PEGylated proteins using enzyme-linked immunosorbant assay (ELISA). In a direct ELISA, the 54.6 kDa EG9 exendin-C-POEGMA conjugate and various controls, including two FDA-approved drugs, Adagen (a PEGylated adenosine deaminase for treating severe combined immunodeficiency disease (SCID)) and Krystexxa (a PEGylated uricase for treating chronic refractory gout), were directly coated on a plate and probed with diluent, an anti-PEG-negative patient plasma sample, or one of two anti-PEG-positive patient plasma samples. As shown in Fig. 5a, although the EG9 exendin-C-POGEMA conjugate did show a small amount of binding to anti-PEG antibodies in the positive plasma samples, the extent of binding was significantly less than those of the two PEGylated-positive controls. This result was confirmed by a competitive ELISA, where Krystexxa was coated on wells, and different amounts of 54.6 kDa EG9 exendin-C-POEGMA and controls were added in solution to compete for binding to anti-PEG antibodies in an anti-PEG-positive plasma sample. As can be seen in Fig. 5b, at all tested competing antigen amounts, the antibody binding of 54.6 kDa EG9 exendin-C-POEGMA was significantly less than that of the positive control, Adagen.

Exendin-C-POEGMA with shorter side-chain length. The previous results led us to hypothesize that the reduced PEG antigenicity of the EG9 exendin-C-POEGMA conjugate is due to both the branched architecture and the short side-chain length of the conjugated POEGMA. As a minimum length of PEG is presumably needed for antibody recognition and binding[42], we hypothesized that optimizing the side-chain OEG length may further reduce or possibly eliminate the antigenicity of POEGMA conjugates to anti-PEG antibodies. To test this hypothesis, we synthesized exendin-C-POEGMA conjugates using OEGMA monomer with precisely three EG side-chain repeats as seen by LC/ESI-MS (Supplementary Fig. 2b), as evidence in the literature suggests that the antigenic determinant of PEG may be approximately six to seven EG repeats[42]. Three different EG3 exendin-C-POEGMA conjugates with M_n values of 26.3, 55.6 and 71.6 kDa (Table 1) were synthesized. Assessment of the

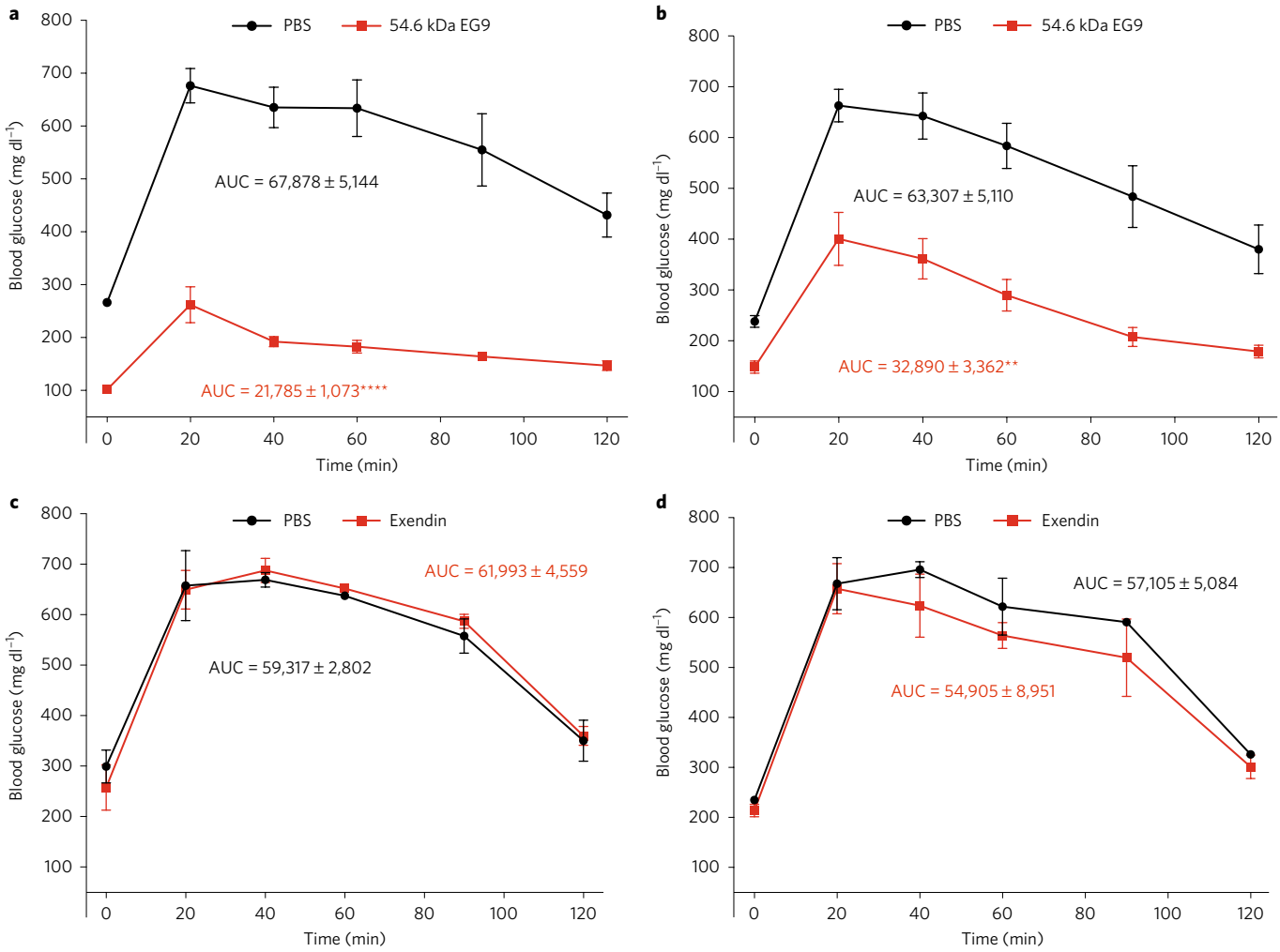

Figure 4 | IPGTT for an EG9 exendin-C-POEGMA conjugate in mice. a–d, Mouse blood glucose levels measured in an IPGTT performed at 24 h (**a**,**c**) and 72 h (**b**,**d**) after a single subcutaneous injection of the 54.6 kDa EG9 exendin-C-POEGMA conjugate or of unmodified exendin at 25 nmol kg^{-1}, compared with PBS of an equivalent volume. Mice were fasted for 6 h before the glucose challenge by an intraperitoneal injection of 1.5 g kg^{-1} of glucose. Results are plotted as mean ± SEM, $n = 5$ in **a**,**b**; $n = 3$ in **c**,**d**. AUCs for the treatment and PBS were compared using an unpaired parametric two-tailed *t*-test (**$P < 0.01$; ****$P < 0.0001$). Differences between the AUCs of PBS and exendin were not significant at either time point.

conjugate potency by intracellular cAMP ELISA (Supplementary Fig. 7) showed that, similarly to the EG9 conjugates, conjugation of EG3 POEGMA to the C-terminus of exendin increased the EC_{50} (Table 1), indicating a decrease in the receptor activation of the conjugates, although the dependence on M_w was less pronounced.

Antigenicity and efficacy of EG3 exendin-C-POEGMA conjugates. We next tested the reactivity of a 55.6 kDa EG3 exendin-C-POEGMA conjugate to anti-PEG antibodies in patient plasma samples. The 54.6 kDa EG9 conjugate was included as a control to confirm the repeatability of the assays. Remarkably, both direct and competitive anti-PEG ELISAs (Fig. 5c,d) showed that reducing the side-chain length of the conjugated POEGMA down to three EG repeats completely eliminated the reactivity of the conjugate towards the anti-PEG antibodies present in the patient plasma samples.

As the OEG side chains on POEGMA are largely responsible for the 'stealth' behaviour of the polymer and its conjugates, alteration of the side-chain length can thus have an impact on the *in vivo* behaviour of POEGMA conjugates. Therefore, we next investigated the *in vivo* efficacy of EG3 exendin-C-POEGMA. The 55.6 kDa and 71.6 kDa EG3 exendin-C-POEGMA conjugates were administered to fed mice via a single subcutaneous injection at 25 nmol kg^{-1} of mouse body weight. As can be seen from the post-injection glucose profiles in Fig. 6a,b (unnormalized glucose profiles and weight profiles in Supplementary Fig. 8), both conjugates significantly reduced mouse blood glucose for up to 96 h compared with the PBS control. The EG3 conjugates seem to have slightly lower magnitudes of glucose reduction and flatter glucose profiles than their EG9 counterparts.

Pharmacokinetics of exendin-C-POEGMA conjugates. To further confirm the prolonged circulation of exendin-C-POEGMA conjugates and to seek some reasons for the difference between the glucose profiles of EG9 and EG3 conjugates, a pharmacokinetics study was performed with fluorescently labelled exendin, and the 54.6 kDa EG9, 55.6 kDa EG3 and 71.6 kDa EG3 conjugates. Two M_w values of the EG3 conjugate were tested, as the EG3 and EG9 conjugates have different hydrodynamic radii (R_h) at the same M_w. These M_w values were chosen such that the 54.6 kDa EG9 conjugate ($R_h = 5.4 \pm 0.6$ nm) had an M_w similar to that of the 55.6 kDa EG3 conjugate and an R_h similar to that of the 71.6 kDa EG3 conjugate ($R_h = 5.6 \pm 0.5$ nm). The plasma-concentration–time courses (Fig. 6c,d) were analysed using a non-compartmental fit that characterized the absorption and

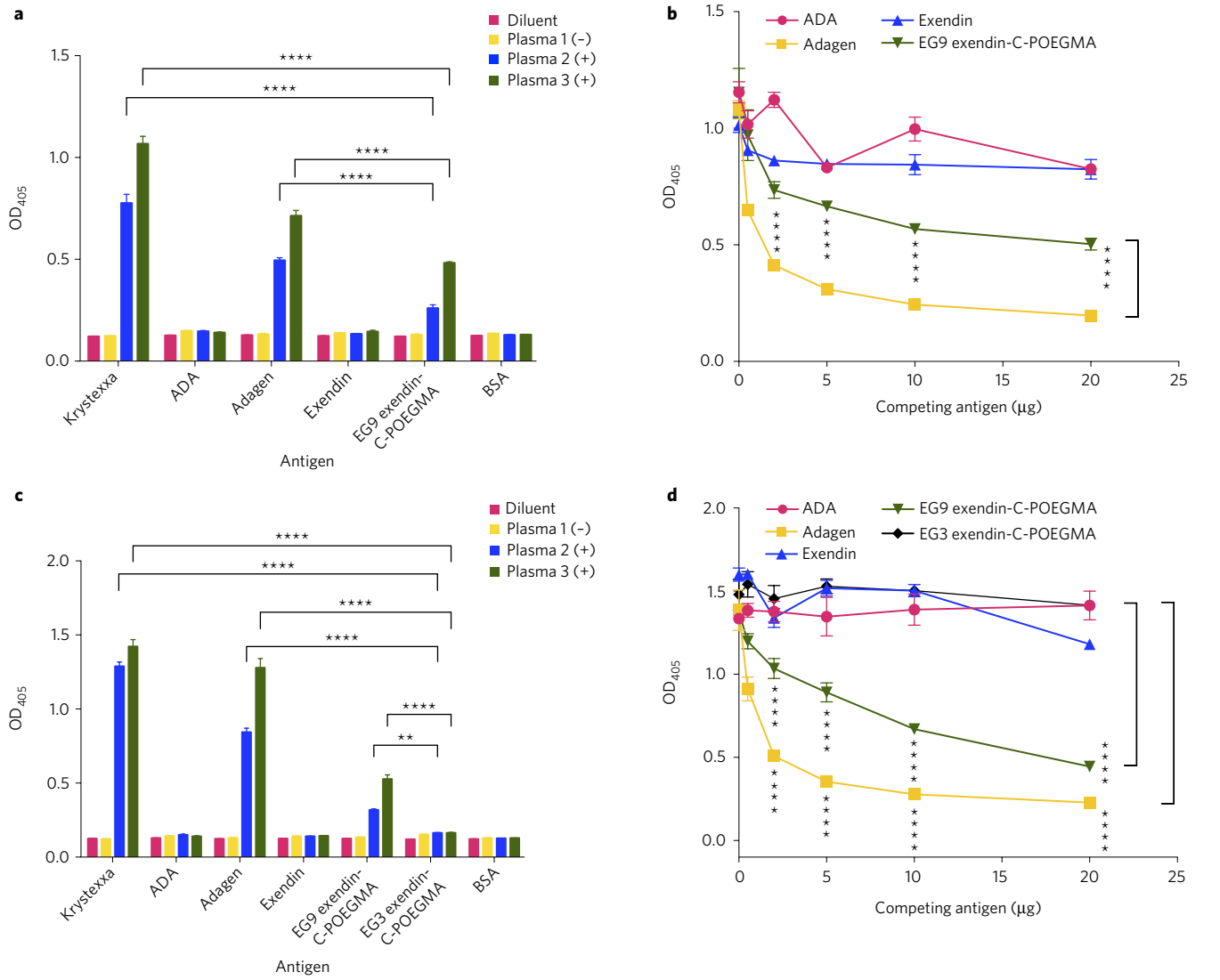

Figure 5 | Assessment of the reactivity of exendin-C-POEGMA conjugates towards anti-PEG antibodies in patient plasma samples. a, Direct ELISA probing 54.6 kDa EG9 exendin-C-POEGMA conjugate, native exendin, ADA, BSA, Krystexxa and Adagen with diluent (1% BSA in PBS), an anti-PEG negative patient plasma sample, or one of two anti-PEG positive plasma samples. **b**, Competitive ELISA, where various amounts of exendin, 54.6 kDa EG9 exendin-C-POEMGA, ADA and Adagen were allowed to compete with Krystexxa for binding with anti-PEG antibodies in a positive plasma sample. **c**,**d**, Direct (**c**) and competitive (**d**) assays as described in **a** and **b** performed with a 55.6 kDa EG3 exendin-C-POEGMA conjugate. In all assays, the same unmodified peptide/protein content or similar PEG/OEG content in the case of polymer-modified samples per well were compared. See Methods section for details. Results are plotted as mean ± SEM, $n=3$ in **a**,**b**; $n=5$ in **c**,**d**. Data were analysed by two-way ANOVA followed by *post hoc* Dunnett's multiple comparison test (**$P<0.01$; ****$P<0.0001$). OD_{405}, optical density at 405 nm.

elimination phases of the pharmacokinetic profiles to approximate the parameters shown in Table 2.

After subcutaneous injection, unmodified exendin had a very short residence time in circulation, with a short absorption half-life ($t_{½a}=0.7\pm0.1$ h) and a short terminal elimination half-life ($t_{½el}=1.7\pm0.2$ h). In contrast, the exendin-C-POEGMA conjugates tested increased the absorption time by ~9-fold to 13-fold, with the two EG3 conjugates taking longer than the EG9 conjugate to absorb into circulation. Similarly, the 54.6 kDa EG9 conjugate prolonged the elimination phase of exendin by ~25-fold, whereas the two EG3 conjugates afforded a bigger increase of ~36-fold. These differences in the pharmacokinetics resulted in an ~20-fold increase in the AUC for the conjugates compared with unmodified exendin, indicating that conjugation of POEGMA to the C-terminus of exendin significantly enhanced the cumulative exposure of the peptide in circulation. Although the peak drug concentrations in plasma (C_{max}) of the two EG3 conjugates were lower than that of the EG9 conjugate, consistent with the lower magnitude of glucose reduction seen for the EG3 conjugates in the blood glucose studies in fed mice (Fig. 6a,b), the AUCs of the three tested conjugates were comparable given the longer absorption and elimination half-lives of the EG3 conjugates.

Discussion

Using our previously developed sortase-catalysed polymer conjugation strategy[22], we synthesized site-specific (C-terminal) and stoichiometric (1:1) exendin-C-POEGMA conjugates with an average overall yield of up to >70%, which compares favourably with the 10–20% overall yield often seen in conventional PEGylation processes[11]. The small fraction of unreacted exendin-C-Br in the *in situ* ATRP reactions is probably due to hydrolysis or disproportionation at the C-terminus of the macroinitiator, which are common

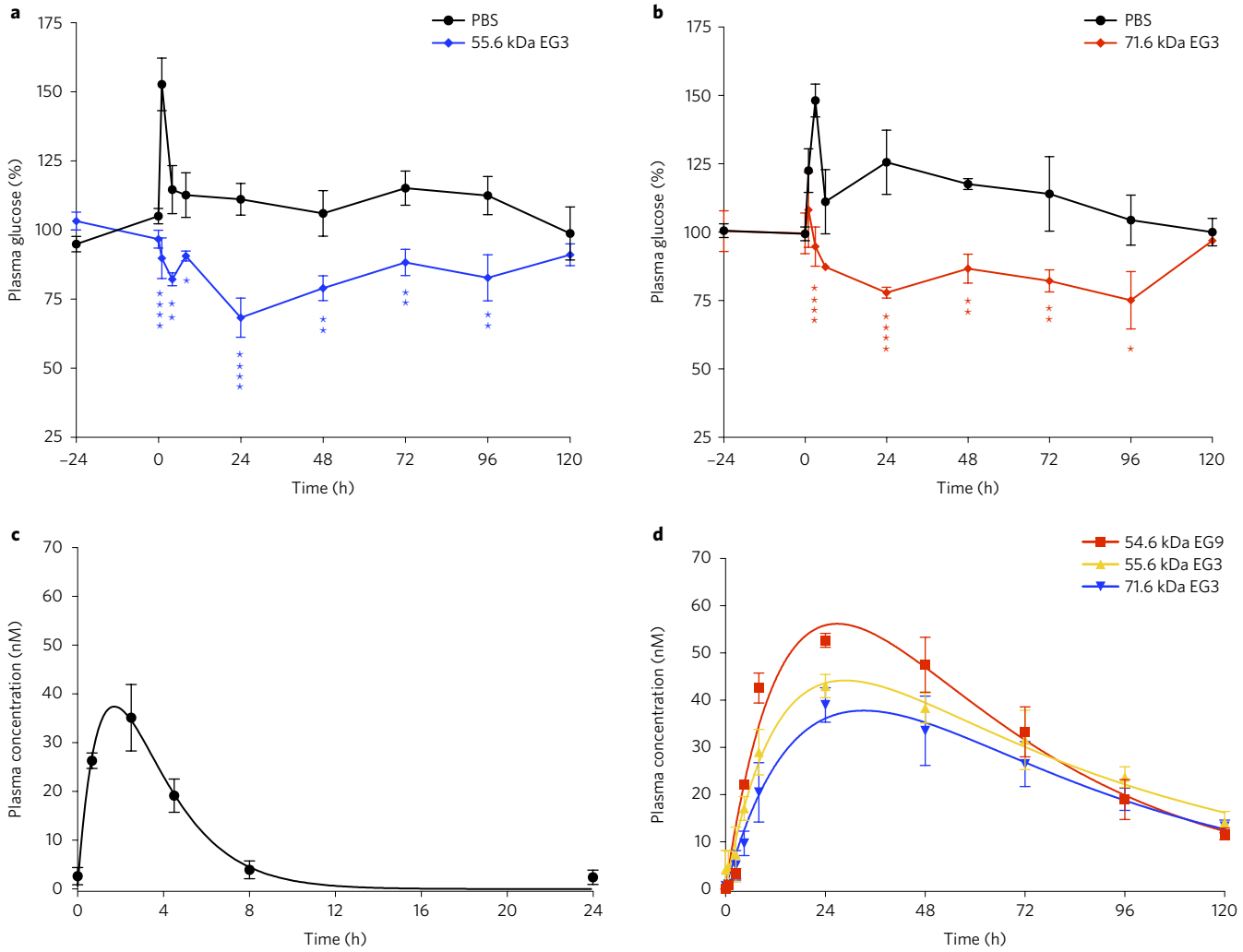

Figure 6 | Assessment of the *in vivo* efficacy and pharmacokinetics of exendin-C-POEGMA conjugates. a,**b**, Blood glucose levels in fed mice measured before and after a single subcutaneous injection of 55.6 kDa (**a**) and 71.6 kDa (**b**) EG3 exendin-C-POEGMA conjugates at 25 nmol kg^{-1} or of PBS at equivalent volume, all administered at $t = 0$ h. Blood glucose levels were normalized to the average glucose levels measured 24 h before and immediately before injection. Data were analysed by two-way repeated-measures ANOVA followed by *post hoc* Dunnett's multiple comparison test ($n = 5$). *$P < 0.05$; **$P < 0.01$; ****$P < 0.0001$. **c**,**d**, Exendin (**c**) and exendin-C-POEGMA conjugates (**d**) were fluorescently labelled with Alexa Fluor 488 and injected into mice ($n = 3$) subcutaneously at 75 nmol kg^{-1} (45 nmol kg^{-1} fluorophore). Blood samples were collected via the tail vein at various time points for fluorescence quantification. Data were analysed using a non-compartmental fit (solid lines) to derive the pharmacokinetic parameters shown in Table 2. Results in all panels are plotted as the mean ± SEM.

side reactions of ATRP in aqueous conditions that lead to loss of Br functionality and thus inactivation of the macroinitiator[43]. Additionally, as a controlled radical-polymerization technique, ATRP enabled the synthesis of conjugates with a wide and tunable range of M_w values and very narrow M_w distributions. Together, our synthesis approach gives rise to polymer conjugates of therapeutic biomolecules that are far more homogeneous than PEGylated drugs that are now in clinical use. This full control over the site and stoichiometry of conjugation, and the high degree of M_w tunability and low dispersity, are highly desirable features for polymer conjugates of therapeutic biomolecules, as they translate to a more predictable therapeutic performance.

EG9 exendin-C-POEGMA conjugates lowered blood glucose levels in fed mice for up to 20 times longer than unmodified exendin injected at the same dose. This prolonged duration of the therapeutic effect substantially reduces the required administration

Table 2 | Pharmacokinetic parameters of exendin and the exendin-C-POEGMA conjugates, calculated from data in Fig. 6c,d.

Exendin/conjugates	$t_{1/2a}$ (h)	$t_{1/2el}$ (h)	C_{max} (nM)*	t_{max} (h)*	AUC (h × nM)†
Exendin	0.7 ± 0.1	1.7 ± 0.2	37.1 ± 3.8	1.78 ± 0.1	217.5 ± 36.5
54.6 kDa EG9	6.2 ± 0.5	42.4 ± 2.9	56.4 ± 3.9	27.1 ± 0.4	4,795.5 ± 440.7
55.6 kDa EG3	7.6 ± 0.7	61.2 ± 5.0	44.0 ± 2.7	28.5 ± 2.3	4,775.0 ± 482.9
71.6 kDa EG3	9.0 ± 1.7	61.5 ± 3.2	37.7 ± 5.0	32.4 ± 3.9	4,411.2 ± 499.6

*Derived from curve fitting. †Calculated from $t = 0$ to ∞ from curve fitting. Values are reported as mean ± SEM. t_{max}: time required to attain C_{max}.

frequency, a benefit that is critical to a disease whose treatment outcomes rely heavily on patient compliance. The blood glucose study of the EG9 conjugates showed that an increase in M_w was correlated with a slower onset of glucose reduction, and that the two higher M_w conjugates provided an overall smaller magnitude of glucose reduction. We speculate that these findings result from, in part, the reduced receptor binding activity and also perhaps a retarded diffusion from the subcutaneous space into systemic circulation, both affected by an increase in conjugate size.

The trends observed in blood glucose levels are also evident in mouse body-weight profiles. A drop in body weight at the beginning of the study is expected for all mice, including for the PBS control group, as the mice are subjected to stress factors including injection and repetitive tail-vein glucose measurements. This stress-induced response is also evident in the sharp spike in their glucose levels at the initial time points. The PBS group in the blood glucose measurement study of the 71.6 kDa EG3 exendin-C-POEGMA conjugate had a more pronounced weight drop than in the other glucose studies. This is probably because mice in these studies were fed a 60 kcal% fat diet, which makes them metabolically less stable, and weight variations are thus more common. The slightly higher weight loss in the PBS group in this particular experiment is consistent with a more sustained initial increase in blood glucose, suggesting that this batch of mice reacted more strongly to the procedural stress.

Two critical—and opposing—features of protein–polymer conjugates that are clearly illustrated by this study are the inverse relationships between conjugate M_w and potency versus circulation duration. Up to a threshold value, the M_w of the conjugate is expected to be directly proportional to the circulation duration but inversely proportional to the receptor-binding activity of the biomolecule of interest. Plotting the AUC of blood glucose profiles of the tested EG9 exendin-C-POEGMA conjugates as a function of conjugate M_n, which accounts for both the magnitude and the duration of glucose reduction, gives an inverted bell-shaped distribution with a minimum at 54.6 kDa, suggesting that the 54.6 kDa conjugate is the optimal among the tested conjugates in terms of balancing receptor-activation potency and sustained duration of action. The result also suggests that the renal clearance threshold for these EG9 conjugates is between 25.4 and 54.6 kDa; although the 25.4 kDa conjugate is more potent than the 54.6 kDa conjugate *in vitro*, its overall glucose-lowering effect is smaller than that of the 54.6 kDa conjugate, and its effect also diminished more quickly, which indicates a much faster renal clearance.

The antigenicity of EG9 exendin-C-POEGMA conjugates, or their reactivity towards pre-existing anti-PEG antibodies in patients, was of particular interest because the serious consequences of PEG immunogenicity have become increasingly apparent. Anti-PEG antibodies have been induced in patients treated with PEGylated drugs and have been shown to correlate with rapid clearance of these drugs[16–18]. High levels of pre-existing anti-PEG antibodies have also been found in individuals who are naive to PEGylated agents and are associated with serious and sometimes life-threatening first-exposure allergic reactions[21]. Therefore, prescreening for polymer conjugates of therapeutic peptides and proteins for antigenicity towards anti-PEG antibodies is crucial.

We found that the 54.6 kDa EG9 exendin-C-POEGMA conjugate showed significantly less reactivity towards anti-PEG antibodies in patient plasmas than Adagen and Krystexxa. More intriguingly, reducing the side-chain length of the conjugated POEGMA to three EG repeats completely eliminated antibody binding. We speculate that the complete elimination of the anti-PEG antigenicity of EG3 POEGMA has two potential molecular explanations. First, three EG repeats may be shorter than the epitope recognized by anti-PEG antibodies, which is consistent with a previous report that the antigenic determinant of PEG may be six to seven repeat units[42]. Second, distributing PEG as oligomeric side chains may create a 'stacking effect' that hinders antibody access. Given that POEGMA is not present in any current pharmaceutical or consumer product, it is reasonable to speculate that humans would not have any pre-existing antibodies to the polymer. Thus, clinically, the lack of anti-PEG antigenicity of POEGMA conjugates is expected to translate to the complete elimination of serious and sometimes life-threatening first-exposure allergic reactions in patients towards POEGMA conjugates of therapeutics, and should eliminate the accelerated blood clearance of POEGMA–drug conjugates due to pre-existing anti-PEG antibodies in patients. We believe this is a particularly timely and useful finding that will address the pressing problem of increasing levels of pre-existing anti-PEG antibodies in the general population, which is compromising the safety and efficacy of FDA-approved PEGylated drugs and hindering the progress of other PEG conjugates in clinical and pre-clinical development. Given that PEGylation remains the most widely used technology to extend the half-life and improve the bioavailability of biologic drugs clinically, a method to tackle the emerging problem of antigenicity of PEG by modulation of its architecture—from linear to branched—provides a new approach to solve this problem. We note that this study addresses the anti-PEG antigenicity of POEGMA conjugates of biologic drugs but does not make any claims about their intrinsic immunogenicity. Although immunogenicity is also a crucial aspect regarding the safety of this class of conjugates, a thorough investigation would involve extensive *in vivo* studies performed in multiple species, which is beyond the scope of this study.

Glucose measurement studies confirmed that the elimination of antigenicity did not occur at the cost of *in vivo* efficacy. While the magnitude of glucose reduction of the EG3 conjugates is slightly lower than that of the EG9 conjugates, the glucose profiles resembled that of a sustained-release depot, without the peak-to-valley effect that is often associated with parenteral drug administration and that can cause unwanted side effects. Pharmacokinetic comparison of the 55.6 kDa and 71.6 kDa EG3 conjugates with the 54.6 kDa EG9 conjugate showed that although the C_{max} values of the EG3 conjugates were smaller than those of the EG9 conjugate, their longer absorption and elimination half-lives gave rise to AUCs that are comparable with those of the EG9 conjugate. This finding is consistent with the flatter and steadier glucose profiles of the EG3 conjugates. We speculate that the relatively higher hydrophobicity of EG3 POEGMA may cause its conjugates to remain in the subcutaneous space or lodge in other tissues during their course in circulation for more extended periods of time, thus creating a depot-like effect.

POEGMA was polymerized from the C-terminus of exendin in this study because the N-terminus of the peptide is important for GLP-1R binding and activation[37]. We note that although we have demonstrated the utility of the sortase-catalysed C-terminal polymer conjugation strategy with exendin in this study, it is a generally applicable platform for improving the pharmacological performance of therapeutic proteins and peptides where the C-terminus is not essential for the activity of the biomolecule. For other biologics where the C-terminal end may be critical to its activity, we have developed a complementary N-terminal approach[26]. If both the N- and the C-termini of the peptide/protein are critical to its activity, methods developed by us and other investigators can be used for the site-specific incorporation of an ATRP initiator at solvent-accessible sites within the primary amino acid sequence of the peptide or protein drug[44,45]. These methods collectively offer a general toolbox that should enable site-specific POEGMA conjugation at any desired solvent-accessible site on a peptide or protein.

Collectively, our results establish site-specific POEGMA conjugation as a next-generation PEGylation technology that is highly useful for improving the pharmacological performance of therapeutic biomolecules while providing a solution to the increasing levels of pre-existing anti-PEG antibodies in patients that limit the safety and

efficacy of traditional PEGylated drugs. Although these results are promising, we believe that a deeper understanding of the mechanism of action, and of the efficacy and the safety of exendin-C-POEGMA conjugates—particularly the EG3 variants—is necessary for clinical translation. Future plans include optimizing the M_w of EG3 exendin-C-POEGMA conjugates to maximize efficacy, measuring insulin release, investigating the *in vivo* biodistribution of the conjugates, and studying the long-term parameters of therapeutic efficacy such as glycated haemoglobin (HbA_{1c}), glycated albumin and pancreatic β-cell proliferation to understand the long-term therapeutic potential of exendin-C-POEGMA conjugates. Furthermore, assessment of the intrinsic immunogenicity of exendin-C-POEGMA conjugates is essential to ensure their long-term safety and efficacy for clinical translation.

Methods

Experimental design. All *in vitro* and *in vivo* experiments include suitable controls; where applicable, PBS served as a negative control and unmodified exendin served as a positive control. The sample sizes for *in vivo* studies were chosen on the basis of similar studies conducted previously[46,47]. See the Animal studies section below for details on the animal model used. Mice were randomly grouped before the initiation of each experiment. The investigator was not blinded to group allocation. For the *in vivo* glucose measurement studies in fed mice, mouse blood glucose levels were measured until all of the experimental groups no longer showed statistical significance in glucose reduction compared with the PBS control group. All collected data points were included in the data analysis.

Cloning, expression and purification. All molecular biology reagents were purchased from New England Biolabs unless otherwise specified. The gene encoding exendin in a pMA-T vector was codon-optimized and synthesized by Life Technologies. The first methionine residue encoding the translational start codon in proteins recombinantly expressed in *E. coli* needs to be cleaved post-translationally for proper function and stability of the protein[48]. However, the first amino acid of exendin is a histidine, and our past experience and reports in the literature[48] both suggest that having histidine as the residue that immediately follows methionine prevents proper methionine cleavage. Thus, a di-alanine leader was incorporated at the N-terminus of the peptide to facilitate methionine cleavage. Once *in vivo*, the di-alanine leader can be cleaved by dipeptidyl peptidase 4 (DPP4), an exopeptidase that cleaves N-terminal dipeptides containing proline or alanine as the second residue, to reveal the N-terminus of exendin for GLP-1R binding. The exendin gene was amplified by polymerase chain reaction (PCR), using forward and reverse primers containing NdeI overhangs and with the sequence for srt followed by a His_6-tag incorporated in the reverse primer. The amplified exendin-srt-His_6 fragment was inserted into a modified pET-24a+ vector[49] at an NdeI restriction site immediately upstream of an ELP with the sequence $(VPGVG)_{60}$, to yield exendin-srt-His_6-ELP.

Expression and purification of the quaternary fusion protein followed previously described procedures with minor changes[22]. Briefly, cells were cultured in Terrific Broth (TB; Mo Bio Laboratories, Inc.) supplemented with 45 μg ml^{-1} of kanamycin at 25 °C. Once the optical density at 600 nm (OD_{600}) of the culture reached 0.6, temperature was lowered to 16 °C and isopropyl β-D-1-thiogalactopyranoside (IPTG, AMRESCO) was added to a final concentration of 0.1 mM to induce protein expression. Cells were harvested 15 h post-induction by centrifugation at 700*g* for 10 min and were lysed by sonication on a Misonex Ultrasonic Liquid Processer (Qsonica, LLC) at amplitude 85 for 3 min with cycles of 10 s on and 40 s off. Nucleic acids were removed from the crude extract via addition of 1 vol% polyethyleneimine (PEI, Acros) followed by centrifugation at 4 °C and 21,000*g* for 10 min. The ELP tag enables the purification of the fusion protein by ITC, a nonchromatographic method we previously developed for the purification of ELP fusion proteins that takes advantage of the inverse phase transition behaviour imparted by the ELP[34]. After triggering the inverse phase transition of the fusion by addition of 0.1 M ammonium sulfate, the aggregated proteins were collected by centrifugation at ~30 °C and 21,000*g* for 10 min. The pellet was then resolubilized in cold PBS and the resulting solution centrifuged at 4 °C and 21,000*g* for 10 min to remove any remaining insoluble material. The last two steps were typically repeated once more to obtain a homogeneous protein, as verified by SDS-PAGE. In the final step, the protein was resolubilized in sortase buffer (50 mM Tris, 150 mM NaCl, 10 mM $CaCl_2$, pH adjusted to 7.5) in preparation for sortase-catalysed initiator attachment.

The gene for sortase A with a 59 N-terminal amino acid truncation (previously shown to not affect its transpeptidase activity[50]) and an N-terminal His6-tag in a pET15b vector was available from a previous study. His_6-sortase A was expressed and purified as previously described[22].

Sortase-catalysed initiator attachment and macroinitiator purification. The exendin-C-Br macroinitiator was synthesized and purified following procedures described previously with minor changes[22]. Briefly, a reaction mixture consisting of exendin-srt-His_6-ELP, His_6-sortase A and AEBMP at a 2:1:60 ratio in sortase buffer was incubated at 20 °C for 18 h. After the reaction, a reverse His-tag purification was used to isolate the exendin-C-Br macroinitiator by exploiting the fact that it is the only species in the mixture without a His_6-tag. Purification was performed on an AKTA Purifier (GE Healthcare) equipped with a photodiode detector set at 280 nm and a HisTrap HP column. Elution through the column with PBS yielded pure exendin-C-Br in the eluent while leaving all other unwanted species bound to the resin. The collected exendin-C-Br was dialysed overnight in PBS (pH 7.4) to remove residual free initiator.

Macroinitiator characterization. MALDI-MS was performed on a Voyager-DE Pro mass spectrometer (Life Technologies). Samples at ~25 μM in PBS were diluted 1:10 with 10 mg ml^{-1} sinapinic acid in 90:10 water/acetonitrile, with 0.1 vol% trifluoroacetic acid (TFA) as the ionization matrix. The instrument was operated in linear mode with positive ions generated using an N_2 laser. Ubiquitin was used as a molecular weight standard to calibrate the instrument.

For LC/MS-MS analysis to confirm site specificity of initiator attachment, 100 μl of ~8 μM exendin-C-Br in PBS was solvent-exchanged into 50 mM ammonium bicarbonate (pH 8.0) on a ZebaSpin desalting column (Thermo Fisher Scientific) followed by trypsin (sequencing grade, Promega) digestion at 37 °C for 18 h directly in the column. The digestion mixture was collected via centrifugation, dried by vacuum centrifugation and resuspended in 20 μl 2% acetonitrile and 0.1% formic acid in water. 1 μl of the sample was separated on a NanoAquity ultra-performance liquid chromatography (UPLC, Waters) system equipped with a BEH130 C18 reversed phase column (Waters) using a mobile phase consisting of (A) 0.1% formic acid in water and (B) 0.1% formic acid in acetonitrile. A linear gradient of 5% B to 40% B was performed over 60 min at 400 nl min^{-1}, and the separated peptides were ionized by electrospray ionization (ESI) followed by MS analysis on a Synapt G2 HDMS QToF mass spectrometer (Waters). The top four most abundant ions were selected for MS/MS. Mass spectra were processed with Mascot Distiller (Matrix Science) and then submitted to Mascot searches (Matrix Science) against a SwissProt_Ecoli database appended with the custom exendin-C-Br sequence. Search results were imported into Scaffold (v. 4.0, Proteome Software), and scoring thresholds were set to yield a minimum of 99% protein confidence for protein identification. Extracted ion chromatograms were performed in MassLynx (v. 4.1). Experimental isotope distributions of the brominated C-terminal tryptic peptide were compared with a theoretical isotope distribution modelled in Molecular Weight Calculator (v. 6.49, Pacific Northwest National Laboratory; http://ncrr.pnl.gov/software).

***In situ* ARGET-ATRP.** All chemical reagents were purchased from Sigma Aldrich and used as received unless otherwise specified. EG9 OEGMA monomer ($M_n \approx 500$ Da or approximately nine side-chain EG repeats on average, Sigma Aldrich, #447943) and EG3 OEGMA monomer (triethylene glycol methyl ether methacrylate, 232 Da, Sigma Aldrich, #729841) were passed through a column of basic alumina to remove the inhibitors.

In a typical reaction, 216 μmol of OEGMA and 21.6 μl of a stock solution of 200 mM $CuBr_2$ and 1.6 M tris(2-pyridylmethyl)amine (TPMA) pre-complexed in MilliQ water with 5% dimethylformamide (DMF) were mixed with 1 ml of 500 μM exendin-C-Br in PBS in a Schlenk flask. A 3.2 mM solution of ascorbic acid in MilliQ water was prepared in a separate flask. The two solutions were degassed by bubbling with argon for 30 min, after which ARGET-ATRP was initiated and maintained by continuously injecting the ascorbic acid solution into the reaction medium using a syringe pump at a rate of 1.6 nmol min^{-1}. Polymerization was allowed to proceed for a specified time at 20 °C under argon and was quenched by bubbling with air. Reactions of the EG3 OEGMA were conducted with 443 μmol of the monomer in 20 vol/vol% methanol in PBS while all other conditions remained the same. At the end of the reaction, the reaction mixture was dialysed against PBS overnight to remove residual small-molecule reagents in preparation for downstream characterization and purification.

Characterization of OEGMA monomers. Monomers diluted 1:20,000 in methanol were separated on an Agilent 1100 LC system equipped with a Zorbax Eclipse Plus C18 column (Agilent) using a mobile phase consisting of (A) 0.3% formic acid in water and (B) 0.3% formic acid in acetonitrile. A linear gradient of 50% B to 95% B was performed over 10 min at 50 °C. Separated samples were ionized by ESI followed by MS analysis on an Agilent MSD ion trap mass spectrometer.

Physical characterization of exendin-C-POEGMA conjugates. Analytical SEC was performed on a Shimadzu HPLC system equipped with a UV–visible detector (SPD-10A VP) operating at 280 nm. 50 μl of samples at ~2 mg ml^{-1} were separated on a Protein KW-803 column (Shodex) using 0.1M Tris-HCl (pH 7.4) as mobile phase at 25 °C with a flow rate of 0.5 ml min^{-1}. The conjugation efficiency of *in situ* ATRP from exendin was calculated by quantifying the AUC of peaks detected at 280 nm. The sum of the AUCs of the two peaks (corresponding to the unreacted macroinitiator and the conjugate in each chromatogram) was regarded as 100% and the per cent fraction of the

conjugate peak was calculated as the conjugation efficiency of that particular polymerization reaction.

The fluid line of the analytical HPLC system was connected downstream in series to a DAWN HELEOS II multi-angle light scattering (MALS) detector followed by an Optilab T-rEX refractometer (both from Wyatt Technology) for conducting SEC-MALS analysis. The system was calibrated with toluene and normalized with 2.0 mg ml^{-1} bovine serum albumin (BSA, Pierce). Samples were passed through 0.1 µm filters before injection. The refractive index increment (dn/dc) values of the conjugates were determined on an Anton Paar Abbemat 500 refractometer (Anton Paar). Data were analysed in ASTRA (v. 6.0, Wyatt Technology) to compute M_w, M_n and $Đ$ for the conjugates.

Conjugates were purified by a single round of preparative SEC on an AKTA Purifier equipped with a photodiode detector set at 280 nm and a HiLoad 26/600 Superdex 200 PG column using PBS as mobile phase at 4 °C and a flow rate of 2.0 ml min^{-1}.

Dynamic light scattering was performed on a DynaPro Plate Reader (Wyatt Technology). Samples were prepared at 25 µM and filtered with 0.1 µm filters before analysis. The instrument was operating at a laser wavelength of 831.95 nm, a scattering angle of 90° and at 25 °C. Data were analysed in Dynals mode using Dynamics 6.12.0.3.

General biochemical analysis. The concentrations of the fusion proteins were measured on an ND-1000 Nanodrop spectrophotometer (Thermo Scientific) by UV–visible absorption spectroscopy. The concentrations of exendin and the conjugates for *in vitro* assays and *in vivo* studies were assessed using a Bicinchoninic Acid (BCA, Pierce) assay following manufacturer's instructions. SDS-PAGE analysis of sortase A was performed using precast 4–20% Tris-HCl gels (Bio-Rad). SDS-PAGE analyses of all exendin derivatives were performed using precast Tris/Tricine gels (Bio-Rad). Quantification of the sortase reaction conversion was conducted via a gel densitometry analysis using a built-in function in Image Lab (v. 4.0.1, Bio-Rad).

***In vitro* cAMP ELISA.** The activity of native exendin and conjugates was assessed *in vitro* by quantifying the intracellular cAMP release as a result of GLP-1R activation in BHK cells that were stably transfected with rat GLP-1R (a gift from Drucker group, University of Toronto, Toronto, Canada)[51]. Cells were allowed to reach 70–80% confluence in 24-well plates. Before the assay, ~20 µg of peptide or the equivalent of conjugates were treated with 0.5 µg DPP4 (ProSpect) overnight to remove the di-alanine leader. On the day of the assay, cells were incubated with 3-isobutyl-1-methylxanthineto (IBMX, EMD Millipore) for 1 h to prevent cAMP degradation[52], followed by incubation with varying concentrations (0.001–1,000 nM in log-scale increments) of exendin (Genscript) or conjugates for 10 min to trigger GLP-1R activation. 0.1 M HCl was then added to disrupt the cells and release intracellular cAMP. cAMP concentration was measured via a competitive cAMP ELISA according to the manufacturer's protocol (Enzo Life Sciences). Each sample was assayed in triplicate and data were analysed in Igor Pro (v. 6.2, Wavemetrics) using a Hill equation fit to determine the EC_{50} of each construct[53].

Animal studies. *In vivo* experiments were performed with six-week-old male C57BL/6J mice (stock no. 000664) purchased from Jackson Laboratories. On arrival, the mice were initiated on a 60 kCal% fat diet (#D12492, Research Diets Inc.) to induce a diabetic phenotype. Previous studies have established C57BL/6J mice on a high-fat diet as an adequate model for type 2 diabetes mellitus, as after one week on a high-fat diet, mice exhibit elevated blood glucose, progressively increasing insulin level and severely compromised insulin response and glucose tolerance[38,39]. Mice were housed under controlled light on a 12 h light/12 h dark cycle with free access to food and water. All mice were allowed to acclimate to the high-fat diet and the facility for 10 d before the initiation of the experiments. The mice used for glucose measurements of the EG3 conjugates were maintained on the high-fat diet for three weeks and used at the age of eight weeks. All animal care and experimental procedures were approved by the Duke Institutional Animal Care and Use Committee.

***In vivo* glucose measurements.** The effect of native exendin and the conjugates on blood glucose levels in fed mice was measured following a single subcutaneous injection of each sample. Before blood glucose measurement, the tail was wiped with a sterilizing alcohol solution and wiped dry. A tiny incision was made on the mouse tail vein using a disposable lancet, and the first 1 µl drop of blood was wiped off. The second 1–2 µl blood drop was used for glucose measurement using a hand-held glucometer (AlphaTrack, Abbott). Blood glucose levels were measured 1 d before the experiment. On the day of injection, weights and blood glucose were measured, and a sample solution or PBS control of equivalent volume was injected subcutaneously. Immediately following injection, mice were placed back in the cage with free access to food and water, and blood glucose was measured at 1, 4, 6 (exendin only), 8, 24, 48, 72, 96, 120 and 144 h post-injection. Weights were monitored daily. In the EG9 dose-dependent study, a 66.2 kDa EG9 exendin-C-POEGMA conjugate was injected into mice ($n=3$) at 25, 50 and 85 nmol kg^{-1} of mouse body weight. In the EG9 M_w-dependent study, EG9 conjugates of 25.4, 54.6, 97.2 and 155.0 kDa M_n were injected into mice ($n=6$) at 25 nmol kg^{-1}. In the EG3 glucose study, 55.6 kDa and 71.6 kDa EG3 exendin-C-POEGMA conjugates were injected into mice ($n=5$) at 25 nmol kg^{-1}. Blood glucose levels were normalized by the average glucose levels measured 24 h before and immediately before injection to reflect the per cent change in blood glucose and to correct for transient variations in glucose.

***In vivo* IPGTT.** Mice were randomly divided into groups ($n=5$ in Fig. 4a,b, $n=3$ in Fig. 4c,d). On day 1, every two groups of mice received a subcutaneous injection of either 54.6 kDa EG9 exendin-C-POEGMA conjugate, exendin as positive control, or PBS at equivalent volume as negative control. Exendin and the conjugate were injected at 25 nmol kg^{-1}. 18 h after injection, one group of mice in each category was fasted by removal of food for 6 h. At the end of the fast period (24 h following injection), mice were given 1.5 g kg^{-1} glucose (10 w/vol% sterile glucose solution, Sigma) via intraperitoneal injection. Blood glucose levels were monitored by nicking the tail vein and measuring the glucose level in the blood using a glucometer at 0, 20, 40, 60, 90 and 120 min after glucose administration. At 66 h after injection, the remaining groups of mice were subjected to the same protocol and an IPGTT was similarly performed 72 h following injection.

***In vivo* pharmacokinetics.** Exendin, 54.6 kDa EG9, 55.6 kDa EG3 and 71.6 kDa EG3 exendin-C-POEGMA conjugates were fluorescently labelled with Alexa Fluor 488 NHS ester (Thermo Fisher Scientific) via their solvent accessible primary amines on lysine residues and the N-terminus, according to the manufacturer's protocol. Unreacted free fluorophore was removed using a ZebaSpin desalting column (Thermo Fisher Scientific). Mice were randomly divided into four groups ($n=3$). Animals were weighed before injection. Each group of mice received a single subcutaneous injection of one of the labelled samples at 75 nmol kg^{-1} (45 nmol kg^{-1} fluorophore). Blood samples (10 µl) were collected from the tail vein into 100 µl of a heparin solution (1 kU ml^{-1} in PBS, Sigma Aldrich) at 40 s, 40 min, 2.5 h, 4.5 h, 8 h, 24 h, 48 h, 72 h, 96 h and 120 h after injection. Blood samples were centrifuged at 4 °C and 20,000*g* for 10 min to extract the plasma for fluorescence reading at excitation 485 nm and emission 535 nm on a Victor multilabel plate reader (Perkin Elmer). The plasma concentrations of the constructs as a function of time were fitted using a non-compartmental analysis (PK Solutions 2.0, Summit Research Services) that characterizes the absorption and elimination phases of the profiles to derive the pharmacokinetic parameters.

***In vitro* anti-PEG ELISA.** In the direct ELISA, columns of a 96-well microtiter plate (CoStar) were coated with Krystexxa (Crealta Pharmaceuticals), adenosine deaminase (ADA, Sigma-Tau Pharmaceuticals), Adagen (Sigma-Tau Pharmaceuticals), exendin (Genscript), a 54.6 kDa EG9 exendin-C-POEGMA conjugate, a 55.6 kDa EG3 exendin-C-POEGMA conjugate or BSA (Sigma Aldrich). The antigen solutions for plate coating were prepared in PBS to yield ~2 µg of unmodified peptide/protein or ~5 µg of PEG/OEG in the case of polymer-modified antigens per well on adding 50 µl to each well. The PEG/OEG contents of the polymer-modified antigens were calculated as follows. Krystexxa consists of the tetrameric uricase enzyme (125 kDa total) with 10–11 lysine side-chain amino groups on each of its four subunits reacted with 10 kDa PEG *p*-nitrophenyl carbonate ester[9], giving a PEG content of ~76%. Adagen consists of ADA (40.8 kDa) with 11–17 of its side-chain amino groups on solvent-accessible lysines functionalized with 5 kDa monomethoxy succinyl PEG according to the manufacturer's specifications (Sigma-Tau Pharmaceuticals). For our calculation, we assumed 14 PEG chains per Adagen conjugate on average, giving ~60% PEG content. In the case of the exendin-C-POEGMA conjugates, subtracting the poly(methyl methacrylate) backbone (~17% for EG9 POEGMA and ~37% for EG3 POEGMA) gives an OEG content of ~75% for the 54.6 kDa EG9 conjugate and ~58% for the 55.6 kDa EG3 conjugate. After the coated plate was incubated overnight at 4 °C, it was washed with PBS and all wells were blocked with 1% BSA in PBS. One patient plasma sample previously tested negative for PEG antibody and two that were tested positive were diluted 1:400 vol/vol in 1% BSA in PBS. The two positive patient plasma samples were from two different individuals who developed anti-PEG antibodies during a phase II clinical trial of Krystexxa. Following another round of PBS washing, 100 µl of each diluted plasma sample and 1% BSA in PBS were added to replicate wells of each antigen. The plate was then incubated at room temperature for 2 h. Wells were again washed with PBS, and 100 µl of alkaline phosphatase-conjugated goat anti-human IgG (Sigma) diluted 1:5250 with 1% BSA in PBS was added to each well. After 1 h incubation at room temperature, wells were washed with PBS followed by Tris-buffered saline. Bound alkaline phosphatase was detected by incubating with *p*-nitrophenyl phosphate (Sigma) in accordance with the directions of the supplier. The phosphatase reaction was stopped by adding 50 µl of 10% NaOH per well, and the absorbance at 405 nm was measured on a plate reader (Tecan Infinite M200 Pro, Tecan Austria).

In the competitive ELISA, a microtiter plate was coated with 50 µl of 100 µg ml^{-1} Krystexxa per well by overnight incubation at 4 °C. Various amounts of ADA, Adagen, exendin, a 54.6 kDa EG9 exendin-C-POEGMA conjugate and a 55.6 kDa EG3 exendin-C-POEGMA conjugate were diluted with PBS to yield 0, 0.5, 2, 5, 10 and 20 µg of competing antigen per well on adding 50 µl to each

well. Dilutions of Adagen and the exendin-C-POEGMA conjugates were prepared such that at each competing antigen concentration, similar PEG/OEG contents were compared (as shown in Supplementary Table 3). The diluted competing antigens were mixed with equal volume of a patient plasma sample that tested positive for PEG antibody (diluted 1:200 vol/vol in 1% BSA in PBS) and incubated at 4 °C overnight. The following morning, all wells were washed with PBS then blocked with 1% BSA in PBS. Wells were washed with PBS after blocking, and 100 µl of each concentration of the competing antigen–plasma mixtures was added in replicate wells. After incubation at room temperature for 2 h, alkaline-phosphatase-conjugated IgG was added for colorimetric readout at 405 nm as described above.

Assays in Fig. 5a,b were performed with $n=3$, while those in Fig. 5c,d were performed with $n=5$.

Statistical analysis. Data are presented as means ± standard error of the mean (SEM). Blood glucose levels in glucose measurement studies ($n=6$) were normalized by the average glucose levels measured 24 h before and immediately before injection. Treatment effects on glucose levels were analysed using two-way repeated-measures analysis of variance (ANOVA), followed by *post hoc* Dunnett's multiple comparison test to evaluate individual differences between a treatment and PBS control at each time point. The AUCs of the glucose profiles were compared using one-way ANOVA followed by *post hoc* Tukey's multiple comparison test ($n=6$). To evaluate the AUC of IPGTT ($n=5$), treatment and PBS were compared using an unpaired parametric two-tailed *t*-test. Both direct and competitive anti-PEG ELISAs ($n=3$) were analysed using two-way ANOVA, followed by *post hoc* Dunnett's multiple comparison test to evaluate individual differences between exendin-C-POEGMA and the other groups for each plasma sample (direct) or antigen concentration (competitive). A test was considered significant if the P value was <0.05. Statistical analyses were performed using Prism 6 (GraphPad software Inc.).

Data availability. Source data for the figures in this study are available at figshare with the identifier doi: 10.6084/m9.figshare.3976761 (ref. 54). The authors declare that all other data supporting the findings of this study are available within the paper and its supplementary information.

Received 28 April 2016; accepted 3 October 2016; published 28 November 2016

References

1. Leader, B., Baca, Q. J. & Golan, D. E. Protein therapeutics: a summary and pharmacological classification. *Nat. Rev. Drug Discov.* **7,** 21–39 (2008).
2. Craik, D. J., Fairlie, D. P., Liras, S. & Price, D. The future of peptide-based drugs. *Chem. Biol. Drug Des.* **81,** 136–147 (2013).
3. Peters, T. J. Serum albumin. *Adv. Protein Chem.* **37,** 161–245 (1985).
4. Awai, M. & Brown, E. B. Studies of the metabolism of I-131-labeled human transferrin. *J. Lab. Clin. Med.* **61,** 363–396 (1963).
5. Banga, A. K. *Therapeutic Peptides and Proteins: Formulation, Processing, and Delivery Systems* (CRC, 2015).
6. Caliceti, P. & Veronese, F. M. Pharmacokinetic and biodistribution properties of poly(ethylene glycol)-protein conjugates. *Adv. Drug Deliv. Rev.* **55,** 1261–1277 (2003).
7. Malik, D. K., Baboota, S., Ahuja, A., Hasan, S. & Ali, J. Recent advances in protein and peptide drug delivery systems. *Curr. Drug Deliv.* **2,** 141–151 (2007).
8. Werle, M. & Bernkop-Schnurch, A. Strategies to improve plasma half life time of peptide and protein drugs. *Amino Acids* **30,** 351–367 (2006).
9. Alconcel, S. N. S., Baas, A. S. & Maynard, H. D. FDA-approved poly(ethylene glycol)–protein conjugate drugs. *Polym. Chem.* **2,** 1442–1448 (2011).
10. Nucci, M. L., Shorr, R. G. & Abuchowski, A. The therapeutic value of poly(ethylene glycol)-modified proteins. *Adv. Drug Deliv. Rev.* **6,** 133–151 (1991).
11. Youn, Y. S., Na, D. H. & Lee, K. C. High-yield production of biologically active mono-PEGylated salmon calcitonin by site-specific PEGylation. *J. Control. Release* **117,** 371–379 (2007).
12. Gauthier, M. A. & Klok, H. Peptide/protein–polymer conjugates: synthetic strategies and design concepts. *Chem. Commun.* 2591–2611 (2008).
13. Qi, Y. & Chilkoti, A. Growing polymers from peptides and proteins: a biomedical perspective. *Polym. Chem.* **5,** 266–276 (2014).
14. Gaberc-Porekar, V., Zore, I., Podobnik, B. & Menart, V. Obstacles and pitfalls in the PEGylation of therapeutic proteins. *Curr. Opin. Drug Discov. Devel.* **11,** 242–250 (2008).
15. Veronese, F. M. Peptide and protein PEGylation: a review of problems and solutions. *Biomaterials* **22,** 405–417 (2001).
16. Ganson, N. J., Kelly, S. J., Scarlett, E., Sundy, J. S. & Hershfield, M. S. Control of hyperuricemia in subjects with refractory gout, and induction of antibody against poly(ethylene glycol) (PEG), in a phase I trial of subcutaneous PEGylated urate oxidase. *Arthritis Res. Ther.* **8,** R12–R22 (2006).
17. Hershfield, M. S. *et al.* Induced and pre-existing anti-polyethylene glycol antibody in a trial of every 3-week dosing of pegloticase for refractory gout, including in organ transplant recipients. *Arthritis Res. Ther.* **16,** R63 (2014).
18. Armstrong, J. K. *et al.* Antibody against poly(ethylene glycol) adversely affects PEG-asparaginase therapy in acute lymphoblastic leukemia patients. *Cancer* **110,** 103–111 (2007).
19. Richter, A. W. & Akerblom, E. Polyethylene glycol reactive antibodies in man: titer distribution in allergic patients treated with monomethoxy polyethylene glycol modified allergens or placebo, and in healthy blood donors. *Int. Arch. Allergy Appl. Immunol.* **74,** 36–39 (1984).
20. Garay, R. P., El-Gewely, R., Armstrong, J. K., Garratty, G. & Richette, P. Antibodies against polyethylene glycol in healthy subjects and in patients treated with PEG-conjugated agents. *Expert Opin. Drug Deliv.* **9,** 1319–1323 (2012).
21. Ganson, N. J. *et al.* Pre-existing anti-PEG antibody linked to first-exposure allergic reactions to Pegnivacogin, a PEGylated RNA aptamer. *J. Allergy Clin. Immunol.* **137,** 1610–1613 (2016).
22. Qi, Y., Amiram, M., Gao, W., McCafferty, D. G. & Chilkoti, A. Sortase-catalyzed initiator attachment enables high yield growth of a stealth polymer from the C terminus of a protein. *Macromol. Rapid Commun.* **34,** 1256–1260 (2013).
23. Matyjaszewski, K. & Tsarevsky, N. V. Macromolecular engineering by atom transfer radical polymerization. *J. Am. Chem. Soc.* **136,** 6513–6533 (2014).
24. Matyjaszewski, K. & Xia, J. Atom transfer radical polymerization. *Chem. Rev.* **101,** 2921–2990 (2001).
25. Bontempo, D. & Maynard, H. D. Streptavidin as a macroinitiator for polymerization: in situ protein-polymer conjugate formation. *J. Am. Chem. Soc.* **127,** 6508–6509 (2005).
26. Gao, W. *et al.* In situ growth of a stoichiometric PEG-like conjugate at a protein's N-terminus with significantly improved pharmacokinetics. *Proc. Natl Acad. Sci. USA* **106,** 15231–15236 (2009).
27. Gao, W., Liu, W., Christensen, T., Zalutsky, M. R. & Chilkoti, A. In situ growth of a PEG-like polymer from the C terminus of an intein fusion protein improves pharmacokinetics and tumor accumulation. *Proc. Natl Acad. Sci. USA* **107,** 16432–16437 (2010).
28. Peeler, J. C. *et al.* Genetically encoded initiator for polymer growth from proteins. *J. Am. Chem. Soc.* **132,** 13575–13577 (2010).
29. Lele, B. S., Murata, H., Matyjaszewski, K. & Russell, A. J. Synthesis of uniform protein-polymer conjugates. *Biomacromolecules* **6,** 3380–3387 (2005).
30. Ryan, S. M. *et al.* PK/PD modelling of comb-shaped PEGylated salmon calcitonin conjugates of differing molecular weights. *J. Control. Release* **149,** 126–132 (2011).
31. Magnusson, J. P., Bersani, S., Salmaso, S., Alexander, C. & Caliceti, P. *In situ* growth of side-chain PEG polymers from functionalized human growth hormone—a new technique for preparation of enhanced protein-polymer conjugates. *Bioconjugate Chem.* **21,** 671–678 (2010).
32. Lovshin, J. A. & Drucker, D. J. Incretin-based therapies for type 2 diabetes mellitus. *Nat. Rev. Endocrinol.* **5,** 262–269 (2009).
33. Boekhorst, J., de Been, M. W., Kleerebezem, M. & Siezen, R. J. Genome-wide detection and analysis of cell wall-bound proteins with LPxTG-like sorting motifs. *J. Bacteriol.* **187,** 4928–4934 (2005).
34. Meyer, D. E. & Chilkoti, A. Purification of recombinant proteins by fusion with thermally-responsive polypeptide. *Nat. Biotechnol.* **14,** 1112–1115 (1999).
35. Mao, H., Hart, S. A., Schink, A. & Pollok, B. A. Sortase-mediated protein ligation: a new method for protein engineering. *J. Am. Chem. Soc.* **126,** 2670–2671 (2004).
36. Jakubowski, W. & Matyjaszewski, K. Activators regenerated by electron transfer for atom-transfer radical polymerization of (meth)acrylates and related block copolymers. *Angew. Chem. Int. Ed.* **45,** 4482–4486 (2006).
37. Goke, R. *et al.* Exendin-4 is a high potency agonist and truncated exendin-(9-39)-amide an antagonist at the glucagon-like peptide 1-(7-36)-amide receptor of insulin-secreting beta-cells. *J. Biol. Chem.* **268,** 19650–19655 (1993).
38. Winzell, M. S. & Ahren, B. The high-fat diet-fed mouse: a model for studying mechanisms and treatment of impaired glucose tolerance and type 2 diabetes. *Diabetes* **53,** S215–S219 (2004).
39. Surwit, R. S., Kuhn, C. M., Cochrane, C., McCubbin, J. A. & Feinglos, M. N. Diet-induced type II diabetes in C57BL/6J mice. *Diabetes* **37,** 1163–1167 (1988).
40. Mack, C. M. *et al.* Antiobesity action of peripheral exenatide (exendin-4) in rodents: effects on food intake, body weight, metabolic status and side-effect measures. *Int. J. Obes.* **30,** 1332–1340 (2006).
41. Kanoski, S. E., Rupperecht, L. W., Fortin, S. M., De Jonghe, B. C. & Hayes, M. R. The role of nausea in food intake and body weight suppression by peripheral GLP-1 receptor agonists, exendin-4 and liraglutide. *Neuropharmacology* **62,** 1916–1927 (2012).
42. Richter, A. W. & Akerblom, E. Antibodies against polyethylene glycol produced in animals by immunization with monomethoxy polyethylene glycol modified proteins. *Int. Arch. Allergy Appl. Immunol.* **70,** 124–131 (1983).

43. Tsarevsky, N. V., Pintauer, T. & Matyjaszewski, K. Deactivation efficiency and degree of control over polymerization in ATRP in protic solvents. *Macromolecules* **37,** 9768–9778 (2004).
44. Averick, S. *et al.* Protein-polymer hybrids: conducting ARGET ATRP from a genetically encoded cleavable ATRP initiator. *Eur. Polym. J.* **49,** 2919–2924 (2013).
45. Bellucci, J. J., Bhattacharyya, J. & Chilkoti, A. A noncanonical function of sortase enables site-specific conjugation of small molecules to lysine residues in proteins. *Angew. Chem. Int. Ed.* **54,** 441–445 (2015).
46. Amiram, M., Luginbuhl, K. M., Li, X., Feinglos, M. N. & Chilkoti, A. Injectable protease-operated depots of glucagon-like peptide-1 provide extended and tunable glucose control. *Proc. Natl Acad. Sci. USA* **110,** 2792–2797 (2013).
47. Schellenberger, V. *et al.* A recombinant polypeptide extends the *in vivo* half-life of peptides and proteins in a tunable manner. *Nat. Biotechnol.* **27,** 1186–1188 (2009).
48. Liao, Y.-D., Jeng, J.-C., Wang, C.-F., Wang, S.-C. & Chang, S.-T. Removal of N-terminal methionine from recombinant proteins by engineered *E. coli* methionine aminopeptidase. *Prot. Sci.* **13,** 1802–1810 (2004).
49. McDaniel, J. R., Mackay, J. A., Quiroz, F. G. & Chilkoti, A. Recursive directional ligation by plasmid reconstruction allows rapid and seamless cloning of oligomeric genes. *Biomacromolecules* **11,** 944–952 (2010).
50. Ilangovan, U., Ton-That, H., Iwahara, J., Schneewind, I. & Clubb, R. T. Structure of sortase, the transpeptidase that anchors proteins to the cell wall of *Staphylococcus aureus*. *Proc. Natl Acad. Sci. USA* **98,** 6056–6061 (2001).
51. Drucker, D. J. & Nauck, M. A. The incretin system: glucagon-like peptide-1 receptor agonists and dipeptidyl peptidase-4 inhibitors in type 2 diabetes. *Lancet* **368,** 1696–1705 (2006).
52. Baggio, L. L., Huang, Q. L., Brown, T. J. & Drucker, D. J. A recombinant human glucagon-like peptide (GLP)-1- albumin protein (Albugon) mimics peptidergic activation of GLP-1 receptor-dependent pathways coupled with satiety, gastrointestinal motility, and glucose homeostasis. *Diabetes* **53,** 2492–2500 (2004).
53. Goutelle, S. *et al.* The Hill equation: a review of its capabilities in pharmacological modelling. *Fundam. Clin. Pharmacol.* **22,** 633–648 (2008).
54. Qi, Y. *et al.* Dataset for A brush-polymer/exendin-4 conjugate reduces blood glucose levels for up to five days and eliminates poly(ethylene glycol) antigenicity. *figshare* http://dx.doi.org/10.6084/m9.figshare.3976761 (2016).
55. Zong, Y., Bice, T. W., Ton-That, H., Schneewind, O. & Narayana, S. V. Crystal structures of *Staphylococcus aureus* sortase A and its substrate complex. *J. Biol. Chem.* **279,** 31383–31389 (2004).
56. Neidigh, J. W., Fesinmeyer, R. M., Prickett, K. S. & Andersen, N. H. Exendin-4 and glucagon-like-peptide-1: NMR structural comparisons in the solution and micelle-associated states. *Biochemistry* **40,** 13188–13200 (2001).

Acknowledgements

The authors thank D.M. Gooden at the Duke Small Molecule Synthesis Facility for the synthesis of AEBMP, E.J. Soderblom at the Duke Proteomics Facility for conducting LC/MS-MS, G. Dubay at the Duke Chemistry Mass Spectrometry Facility for LC/ESI-MS support and M.N. Feinglos for discussion of the *in vivo* results. BHK cells expressing GLP-1R were a gift from the Drucker group (University of Toronto, Canada). This work was supported by the National Institutes of Health (R01-DK092665 to A.C.).

Author contributions

Y.Q. and A.C. conceived and designed the research. Y.Q., A.S., N.J.G., X.L, I.O. and W.L. performed the experiments. A.S. and K.M. provided technical expertise in polymer chemistry. K.M.L. and W.L. contributed to the design of the *in vivo* studies. N.J.G. and M.S.H. provided materials and technical expertise for the antigenicity studies. Y.Q., N.J.G., K.M.L., M.S.H., K.M. and A.C. analysed and interpreted the results. Y.Q. and A.C. wrote the manuscript and A.S., N.J.G., K.M.L., M.S.H. and K.M. edited the manuscript. All authors discussed the results and commented on the manuscript.

Additional information

Supplementary information is available for this paper.

Reprints and permissions information is available at www.nature.com/reprints.

Correspondence and requests for materials should be addressed to A.C.

How to cite this article: Qi, Y. *et al.* A brush-polymer/exendin-4 conjugate reduces blood glucose levels for up to five days and eliminates poly(ethylene glycol) antigenicity. *Nat. Biomed. Eng.* **1,** 0002 (2016).

Competing interests

A.C. and Y.Q. have a pending patent on the sortase-catalysed C-terminal polymer conjugation technology (WO 2014194244 A1). M.S.H. is a co-inventor of Pegloticase (Krystexxa) and receives royalties from sales of Pegloticase, along with his employer, Duke University. The results reported in this paper form the basis of US provisional patent applications (62/270,401; 62/329,800; 62/310,534; 62/407,403) filled by A.C., Y.Q., M.S.H. and N.J.G. through the Duke University Office of Licensing & Ventures.